Modeling of Post-Tensioned Segmental Bridge Components

A group of researchers at the University of California – San Diego Department of Structural Engineering is studying the behavior of post-tensioned segmental concrete bridges under seismic loading. They are doing this with physical testing of bridge components at _ and _ scale. This work is described in a series of articles in the PCI Journal.

Megally, S., F. Seible, M. Garg, & R. Dowell. (2002). "Seismic performance of precast segmental bridge superstructures with internally bonded prestressing tendons," *PCI Journal*, 47(2), p. 40-56.

Megally, S., F. Seible, & R. Dowell. (2003a). "Seismic performance of precast segmental bridges: Segment-to-segment joints subjected to high flexural moments and high shears," *PCI Journal*, 48(3), p. 72-90.

Megally, S., F. Seible, & R. Dowell. (2003b). "Seismic performance of precast segmental bridges: Segment-to-segment joints subjected to high flexural moments and low shears," *PCI Journal*, 48(2), p. 80-96.

Finite Element Modeling:

A 3-d finite element model of one of the test specimens was created in Ansys. This specimen consisted of 6 superstructure segments. The post-tensioning strands were grouted in the end segments and unbonded across the center 4 segments. Figure 1 shows a schematic of the test setup. Figure 2 shows the finite element model of this situation. The concrete was modeled using 8-noded brick elements. Each segment was meshed as a separate volume with 3528 elements. Shear was carried across the interfaces by coupling adjacent nodes. Similar coupling was also used to constrain the segments against relative transverse movement. Contact elements at the interfaces allowed the compression forces to develop at the joints, but eliminated tension forces. In reality, the epoxy between the segments does carry some tension until either the epoxy or the adjacent concrete breaks. The simple contact case created is slightly conservative. The post-tensioning strand was modeled using link elements which resisted only axial forces and provided the tension component necessary to resist the moments created by the loading.

The concrete was assumed to be linear-elastic for the range under consideration. The Young's modulus was estimated using the ACI equation $E=57{,}000\sqrt{f'c}$ and the measured compressive strength of the concrete in the test specimen. A multilinear plasticity model was used for the post-tensioning steel.

Load was applied in three steps. In the first step, the prestressing capabilities of Ansys were used to apply the post-tensioning force. This operation works the same way as the physical post-tensioning operation: the strand is shortened until the desired force is achieved, then it is locked in place. In the second step, the self-weight of the assembly was applied. This is similar to the actual construction sequence, where each segment was supported until after post-tensioning. In the third step, the four actuator forces were applied. Each of these forces was uniformly distributed over a block of nine nodes on the top surface of the segment.

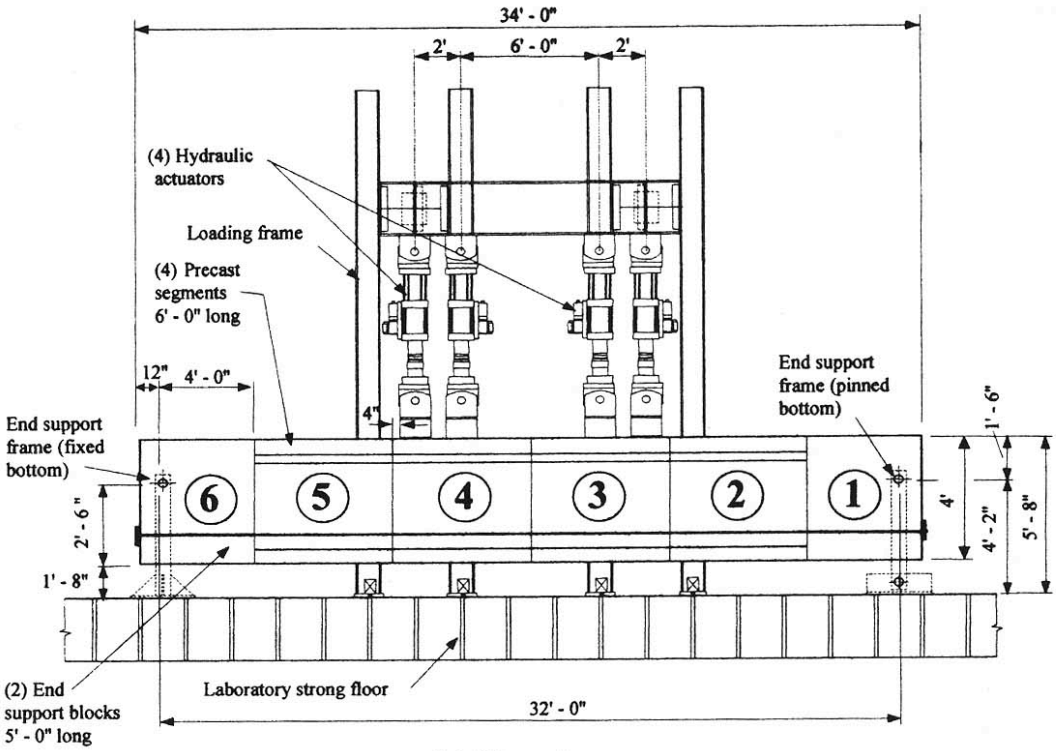

(a) Elevation

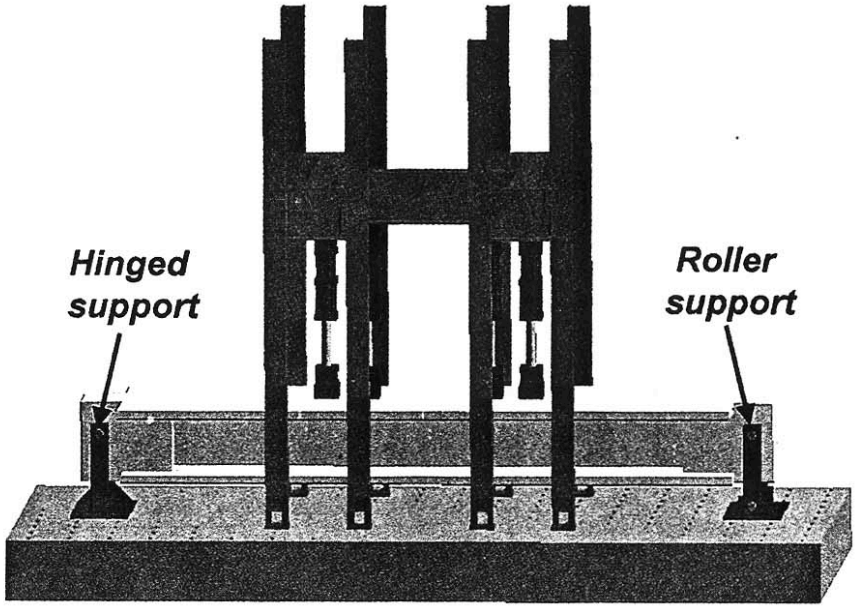

(b) Three-dimensional view

Figure 1. Test setup schematic.
(from Megally, Seible, & Dowell 2003a)

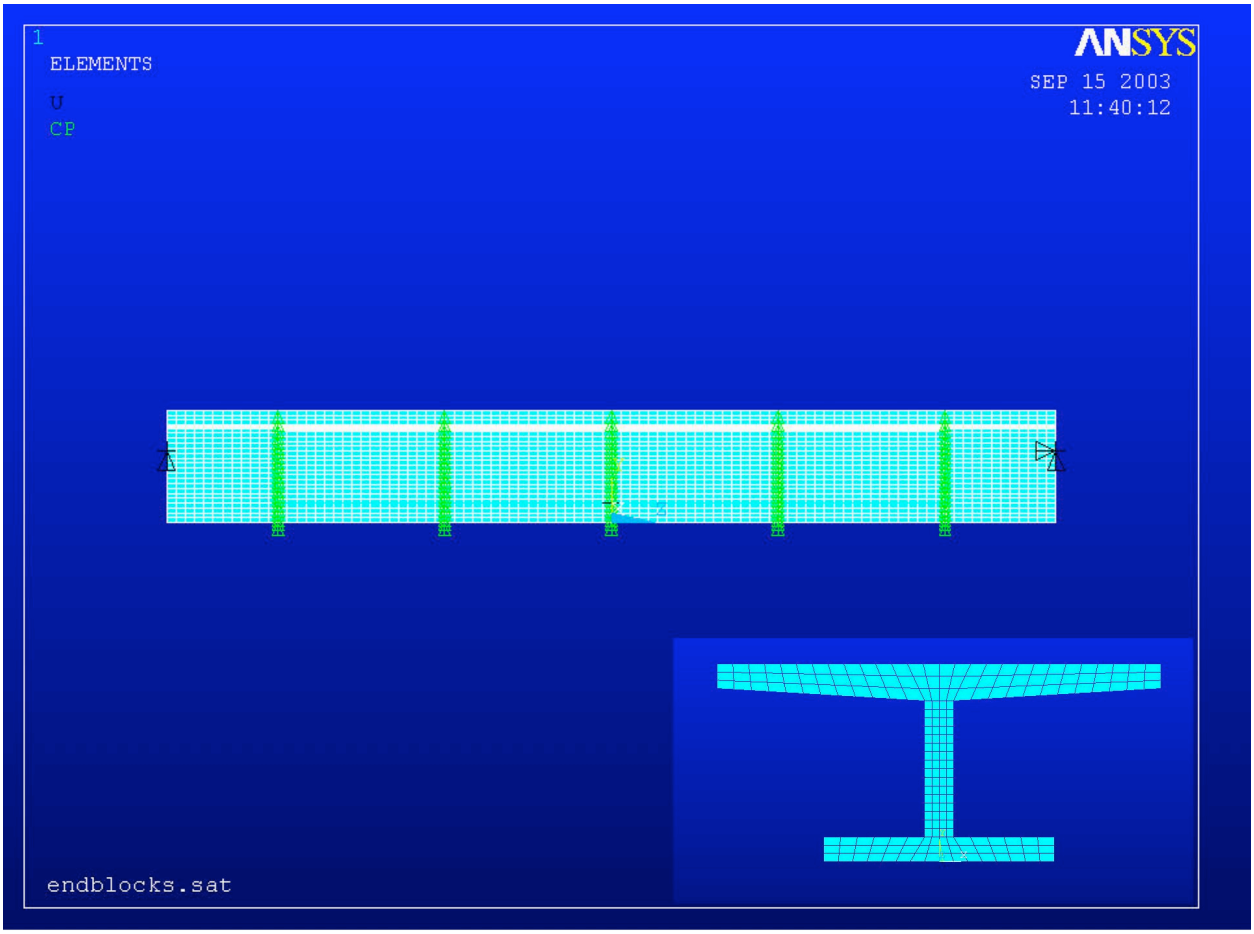

Figure 2. FEM Discretization of the test specimen.

Results and Comparison to Physical Loading:

The results obtained with this model are very similar to the physical test data. Figure 3 shows the deformed specimen with a downward load applied. Figure 4 shows the load-deflection curve of the FE model overlaid on load-deflection curves from the physical testing. The first loop of this curve shows the effect of the tensile capacity of the epoxy connection between the segments. Once the concrete broke near this connection, the loading loop matches the finite element model very well. The subsequent loops show the effects of plastic deformation of the concrete (including crushing) over the course of the loading sequence. The finite element model used a linear-elastic constitutive model for the concrete and did not account for any plastic deformations of the concrete or for crushing of the concrete. While the finite element model does not track exactly with the collected data in this area, the calculated load is within 5% of the measured load for any given displacement. Also, the slopes of the curves are very similar.

The loading on the finite element model was terminated when the opening of the center joint reached a point where the contact area was smaller than the contact elements, which led to mathematical difficulties. Figure 5 shows the contact area at the last solution. A finer mesh would improve this situation to a certain extent. Also, as the joint opened in the physical test, plastic deformation and crushing of the concrete near the top of the deck allowed a larger area to remain in contact. Using a more refined model of the concrete might improve the correlation

between the model and the test results. However, this would lead to a significant increase in the difficulty of the problem. A complete concrete constitutive model would have to be created, and the computational requirements would increase considerably. Assuming that the concrete is linear-elastic leads to a reasonable model with much less expense.

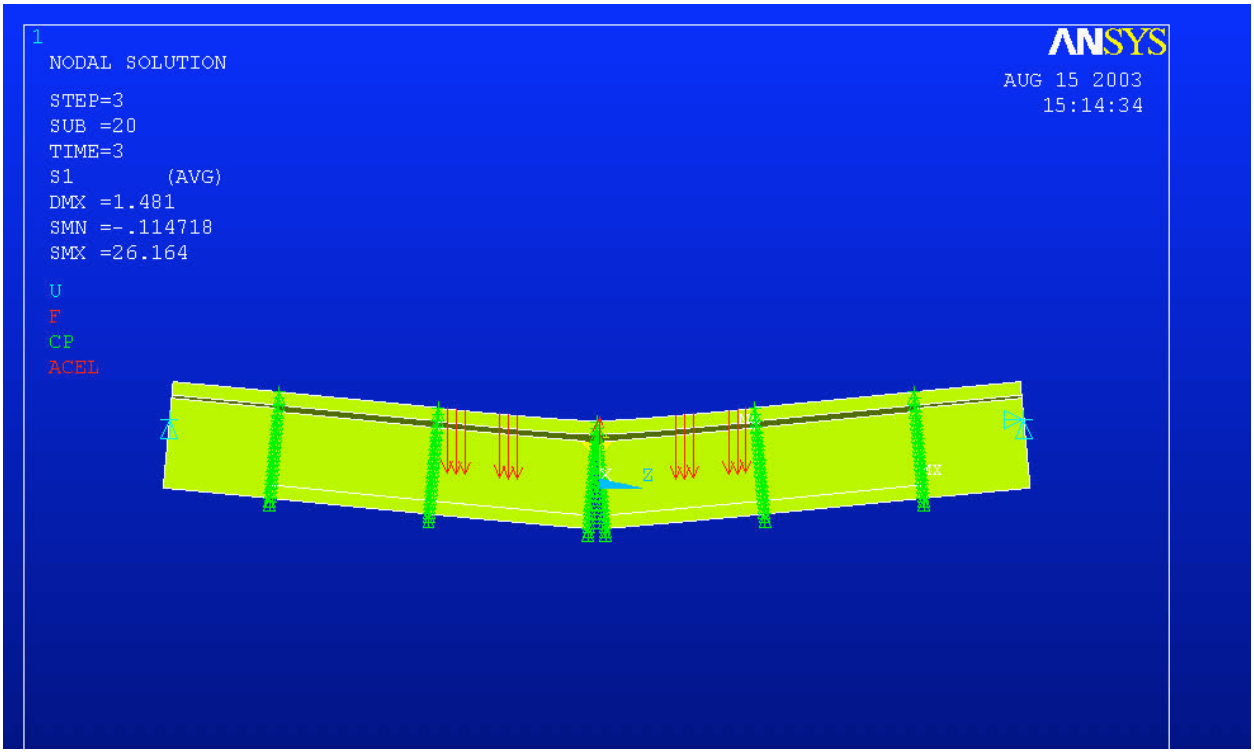

Figure 3. Deformed shape of specimen under downward load.

Figure 4. Load-Deflection plots.

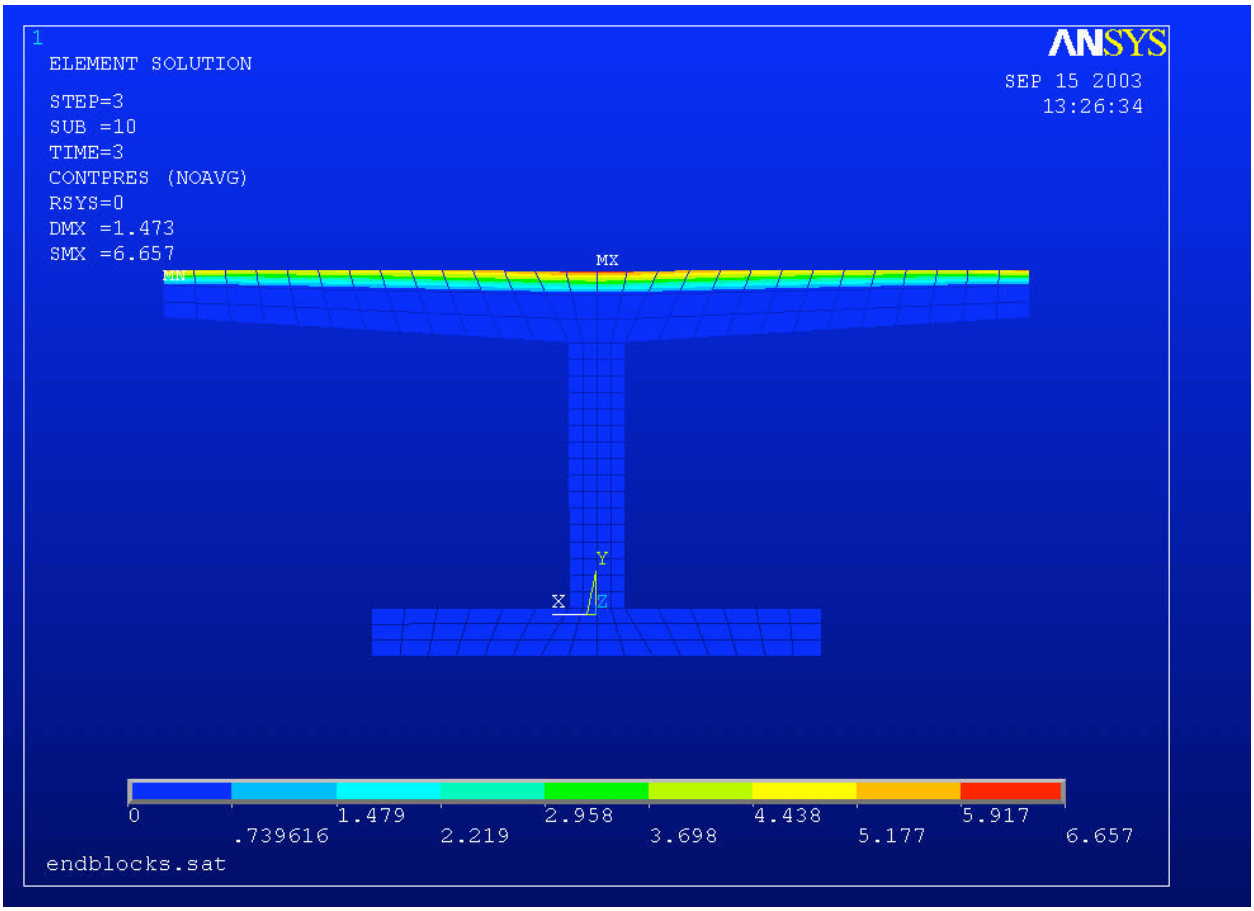

Figure 5. Contact pressure distribution at center joint under maximum downward load.